Carbon Vol. 25, No. 3, pp. 377–389, 1987
Printed in Great Britain.

0008-6223/87 $3.00 + .00

A THEORY FOR THE KINETICS OF INTERCALATION OF GRAPHITE*

S. H. ANDERSON AXDAL and D. D. L. CHUNG
Department of Metallurgical Engineering and Materials Science, Carnegie-Mellon University, Pittsburgh, Pennsylvania 15213, U.S.A.

(*Received* 12 *May* 1986; *in revised form* 12 *September* 1986)

Abstract—A theory, which takes into account the evaporation, transport and condensation of the intercalate outside the graphite and the diffusion and staging inside the graphite, is presented for the kinetics of intercalation of graphite. The theory has been applied to a number of intercalates (including Br_2, ICl, K, Rb, Cs, $FeCl_3$, $NiCl_2$, $CuCl_2$, $PdCl_2$, HNO_3, AsF_5 and SbF_5) at various temperatures. Rate-controlling reaction steps have been identified for different types of intercalation compounds.

Key Words—Intercalation, kinetics, staging, intercalation evaporation, intercalation transportation, intercalation condensation.

1. INTRODUCTION

Presented in this paper is a mechanistic model of the intercalation of graphite. Until recently there has not been a lot of attention paid to the mechanism of intercalation. Hooley[1] performed experiments which indicated that the intercalation of bromine in graphite began near the surface edges of the sample, but that the intercalate was not transported through graphite basal planes. Bardhan and Chung[2] proposed a phenomenological model for the intercalation of bromine in graphite in keeping with Hooley's results; they assumed that the intercalate layers were nucleated at the sample edge at time $n\Delta t$, where n was the number of graphite layers from a free surface and Δt was the time interval between successive nucleation events. The intercalate was considered to be migrating into the sample at a constant velocity. Metz and Siemsgluss[3], investigating the intercalation of ferric chloride, observed that a uniform concentration of iron chloride existed across the sample at very short intercalation times and suggested that the weight gain could be described as a first-order reaction. Dziemianowicz *et al.*[4] proposed that the weight gain during the intercalation of graphite by nitric acid could be described by an exponential nucleation rate term and an effective diffusivity within the graphite. Dowell[5,6] used a Ficksian diffusion approach to describe the intercalation of bromine, nitric acid and palladium chloride.

Other investigators have remarked on the kinetics of intercalation, although specific models may not have been applied. Ubbelohde *et al.*[7] investigated the effect of an external uniaxial pressure on the rate of bromine intercalation, as well as the dependence of the intercalation rate on the graphite quality. Recently several investigators studied in situ the intercalation of alkali metals using gamma rays[8] and X-rays[9].

A theoretical description of staging kinetics has been developed from the seminal work of Safran[10,11]. Extended by the work of Kirczenow[12] and Hawrylak[13], Safran's model of interacting electrostatic and elastic forces appears to offer a valid explanation for the staging process and insight into the kinetics of the staging reaction. For the overall intercalation process, however, this quality of modelling may be inappropriate. On a macroscopic scale intercalation reactions may be better understood if the process of intercalation is divided into individual reaction steps. If this is done, the individual steps can be analyzed to determine their influence on the reaction kinetics.

2. REACTION STEPS

The intercalation process can be broken up into several steps, any of which can be rate controlling depending on the reaction conditions. In general, a reaction may be controlled by a reaction at an interface or by the transport between interfaces. In the particular case of intercalation in the overall reaction may be broken up into several steps:

1. evolution of a transportable species, in the case where the source of the intercalate is a separate phase from the transport medium;
2. transport of the intercalate to the surface of the sample;
3. adsorption of the intercalate onto the surface of the sample from the transport medium;
4. insertion of the intercalate into the sample;
5. transport of the intercalate through the sample;
6. the staging reaction occurring at the interface

*This work was supported by the Air Force Office of Scientific Research, Air Force Systems Command, USAF, under Grant No. AFOSR-78-3536.

between the initial stage and the pristine graphite, or between the initial stage and the previous stage.

While the reactions steps occur concurrently, the steps have an order of progression. E.g., adsorption of the intercalate on the surface cannot occur until transport of the intercalate to the surface of the sample has occurred. If the overall reaction time is of interest, identification of the rate-limiting step, if one exists, is sufficient to approximate the reaction time. For this purpose it is convenient to describe each step in terms of the time involved at each step, so that the total reaction time can be represented as the sum of the times of the various steps. That is,

$$\text{total time for reaction} = \frac{\text{volume intercalate reacted}}{\text{evolution rate}} + \frac{[\text{fluid transport distance}]^2}{\text{fluid diffusion coefficient}} + \frac{\text{volume intercalate reacted}}{\text{adsorption rate}} + \frac{[\text{intercalated length}]^2}{\text{intercalate diffusion coefficient}} + \frac{\text{intercalated length}}{\text{staging reaction rate}}. \quad (1)$$

A certain amount of time is required for each step, and the overall reaction kinetics is determined principally by the slowest or a combination of the slowest steps. The steps can be considered individually to determine the factors pertinent to each step.

3. EVOLUTION OF THE INTERCALATE

In the case where the sample and the intercalate source are physically separate, it is necessary to consider the injection of the intercalate into the medium separating the intercalate and the sample. Typically this would involve evaporation or sublimation of the intercalate. On an atomistic basis, the evaporation rate can be represented as the product of the probability for a molecule to become vapor and the surface area of the intercalate exposed to the transport medium. The evaporation rate may be approximated by [14]

$$\text{evaporation rate} = \frac{1}{r_s^3}\left(\frac{\pi kT}{2m}\right)^{1/2} e\,\frac{-E_e}{RT}, \quad (2)$$

where:

r_s = the intermolecular separation,
E_e = the enthalpy of evaporation, and
m = the molecular mass.

Eq. (2) has been written with the molecular velocity explicitly expanded to show the mass and temperature dependence. The net evaporation rate must also take into account the recondensation of the intercalate onto the parent source from the transport medium. This term is the product of the number of intercalate molecules in the transport phase colliding with the source surface and the probability of a molecule sticking to the surface when this happens[14].

$$\textit{condensation rate} = \frac{\phi n_v}{4}\left(\frac{8kT}{\pi m}\right)^{1/2} \quad (3)$$

where

ϕ = the sticking probability,
and n_v = the number of molecules per unit volume.

The sticking probability can be calculated knowing that, at the vapor pressure, the evaporation rate and the recondensation rate are equal. Hence, if one assumes ideal gas behavior, the sticking probability at the source is [14]

$$\phi = \frac{\pi n_s}{P_v} kTe\,\frac{-E_e}{RT}, \quad (4)$$

where:

$n_s = 1/r_s^3$.

The net rate of intercalate leaving the surface is the difference between the condensation rate and the evaporation rate:

$$\textit{net rate} = n_s\left(\frac{\pi kT}{2m}\right)^{1/2} e\,\frac{-E_e}{RT}\left(1 - \frac{P}{P_v}\right) \quad (5)$$

where:

n_v has been replaced by P/kT.

The evaporation rate is approximately constant until the partial pressure is near the equilibrium vapor pressure.

4. TRANSPORT OF THE INTERCALATE TO THE SAMPLE

Another kinetic step which exists when the sample and intercalate source are separate is the transport of the intercalate to the sample. The form of this kinetic term is dependent on the nature of the transport medium. At very low pressures, gas phase transport kinetics are determined largely by the average molecular velocity. In the presence of an inert atmosphere and high total pressure, the diffusion of the intercalate from the source to the sample dom-

inates this step. The flux of the intercalate may be represented by [15]

$$J = \frac{\alpha_v(P_E - P_S)(2\pi mkT)^{1/2}}{1 + \alpha_v \frac{S}{D}\left(\frac{kT}{2\pi m}\right)^{1/2}} \quad (6)$$

where:

J is the flux of the intercalate,
α_v is a vaporization coefficient which is the ratio between the observed evaporation-rate in vacuum and that calculated from the equilibrium vapor pressure, (For simple substances $\alpha_v \approx 1$)
S is the distance from the intercalate source to the sample,
D is the diffusion coefficient of the intercalate through any gas which may be present,
P_S is the vapor pressure of the intercalate at the sample,
and P_E is the equilibrium vapor pressure of the intercalate.

For fast diffusion ($D/S \gg \alpha_v(kT/2\pi m)^{1/2}$), the pressure of the intercalate at the sample is approximately the equilibrium pressure, and the flux is proportional to the average velocity of the intercalate vapor molecules and the number of intercalate molecules per unit volume. For slow diffusion, the intercalate flux will be proportional to the diffusion coefficient and the pressure gradient between the source and the sample. If more than one component makes up the gas phase, an intermolecular diffusion coefficient may be used which can be calculated as [14]

$$D_{12} = \frac{kT[8kT(m_1 + m_2)]^{1/2}}{3\pi(p_1 + p_2)(\pi m_1 m_2)^{1/2}\,\delta_{12}^2}, \quad (7)$$

where

D_{12} is the interdiffusion coefficient,
m_1 is the mass of a molecule of species 1,
d_{12} is the average effective molecular diameter,
δ_{12}^2 is effective molecular cross-section,
and p_1 is the partial pressure of species 1.

5. ADSORPTION OF THE INTERCALATE ON THE SURFACE

The condensation rate may be rate limiting when the surface is not completely covered by the intercalate. That is, if the coverage of the surface by the intercalate is less than that expected at equilibrium, the chemical potential of the intercalate on the surface will be lower than the chemical potential of the intercalate vapor. At low-intercalate vapor pressures, the adsorption rate, $d\gamma/dt$, can be approximated by [14],

$$\frac{d\dot{\gamma}}{dt} = Ap_x(1 - \theta_s)\gamma_t e^{\frac{-E_a}{kT}}, \quad (8)$$

where:

θ_s is the fraction of surface covered,
γ_t is the total number of adsorption sites on the surface,
$\dot{\gamma}_x$ is the number of sites on the surface which are occupied by x,
p_x is the partial pressure of x,
A is the surface area,
E_a is the heat of adsorption.

With a coverage of more than a monolayer, this equation does not apply. At a coverage of greater than a monolayer, it is more difficult to calculate adsorption rates, but by the same token the presence of a coverage that is greater than a monolayer indicates that the adsorption rate is not rate limiting. At that point the chemical potential of the adsorbed layer is approximately the same as the chemical potential of the vapor. As a first approximation, the chemical potential of the intercalate adsorbed onto the surface was assumed to be approximately equal to that in the vapor phase when the first monolayer was complete. Within that approximation, it should be valid to use this equation to calculate an adsorption rate.

6. NUCLEATION RATES AND SURFACE DIFFUSION

Several processes can occur on the graphite surface to affect the intercalation rate and none of them are particularly tractable. Three primary reaction steps on the surface are nucleation of insertion sites, transport of intercalating species to insertion sites (surface diffusion), and charge transfer between the graphite and the intercalating species. The surface diffusion term is perhaps conceptually the easiest, as it will be proportional to the surface coverage of the intercalating species and inversely proportional to the square of the average distance between insertion sites. While a surface diffusion coefficient can be approximated easily, the coverage and distance terms are intimately related to the other reaction steps. The average distance between insertion sites is determined by the nucleation kinetics. The nucleation rate is expected to have an Arrhenius dependence on two energy terms, a) an activation energy for the transition from the surface state to the intercalated state, and b) a composite energy term due to the change in free energy for the reaction and strain energy and surface energy terms arising from the presence of an intercalated region in the sample. The surface coverage of the intercalating

species is related to the charge transfer rate which forms the intercalating species.

7. TRANSPORT WITHIN THE SAMPLE

Once the intercalate has arrived at the surface of the sample and has been inserted into the sample, there needs to be an accounting of the time spent transporting the intercalate through the sample. As a first approximation, this can be treated as simple diffusion. In particular, if the diffusion distance is considered to be the distance to a particular concentration, e.g., the leading edge of the interface between the intercalated and unintercalated regions, then the diffusion distance will be proportional to the square root of the intercalation time.

$$x = \sqrt{Dt} \tag{9}$$

where:

x is the diffusion distance,
D is an apparent diffusion coefficient,
t is the time allowed for diffusion.

The diffusion coefficient is assumed to be of the form

$$D = D_o \exp[-E_a/RT] \tag{10}$$

where:

D_o is the diffusion coefficient premultiplier, and
E_a is the activation energy for diffusion.

While eq. (10) may be useful for an approximation of the diffusion distance, it does not take into account either the effect of concentration or the existence of multiple stages. A more rigorous approach to diffusion during intercalation can be obtained by using the theory of multiphase binary diffusion of Shatynski *et al.*[16].

Herold[17] has pointed out that two forms of intercalate motion can be considered; diffusion of the intercalate as a molecular species (e.g., the bromine exchange rate measured by Aronson[18]), and the "sliding motion" of the intercalate islands (i.e., the motion responsible for changing stages). In this paper diffusion is considered to be the process whereby the intercalate migrates from the edge of the sample to the interior. As such, it does not distinguish between these two forms of motion.

8. STAGING REACTION

In this paper, the staging reaction is considered to be the process whereby the s^{th} stage is formed from the $(s + 1)^{th}$ stage. X-ray diffraction indicates that the first stage which is formed is not the final stage. Like the insertion of the intercalate, the reaction appears to have first-order kinetics, in the sense that the reaction from stage $s + 1$ to stage s can be written in the form

$$sC_{(s+1)n}I + I = (s + 1)C_{sn}I \tag{11}$$

where s is the final stage, I refers to the intercalate and n is the stoichiometric ratio of I to C in an intercalate layer. The equilibrium constant can then be written as

$$K = \frac{(a_{C_{sn}B})^{s+1}}{(a_{C_{(s+1)n}B})^s (a_B)} = e\frac{\Delta G}{RT}. \tag{12}$$

If the activity of the solid phases are taken to be one—a fairly common approximation—the equilibrium constant is proportional to just the reciprocal of the intercalate activity, or the reciprocal of the fugacity of the intercalate gas phase.

The reaction rate, i.e., the rate of motion of the interface between stages, can be considered to be the probability of an advance of the interface times the driving force of the reaction. The driving force of the reaction can be considered to be the change in free energy due to the formation of the intercalation compound. The chemical potential is often used as a description of the driving force for the reaction, where the chemical potential of component i can be defined as the change in the free energy of phase a with respect to a change in the amount of i, if temperature and pressure remain constant. Then v, the velocity of the intercalate interface, can be written as

$$v = v_o \exp[E_v/RT] (\mu_i^{ext} - \mu_i^{int}) \tag{13}$$

where

v_o is a velocity premultiplier,
E_v is an activation energy for the velocity premultiplier describing the temperature dependence of the velocity,
μ_i^{ext} is the chemical potential of the intercalate external to the sample,
and μ_i^{int} is the chemical potential of the intercalate at the staging interface.

The concept of an interface between stages requires further exposition. It is easy to imagine that within a sample one stage exists alongside another stage. However, if the stages are imagined to be formed by complete sheets of intercalate between graphite planes, difficulties arise in explaining the transition of one stage to another. In particular, Daumas and Herold[19] pointed out that if an intercalation compound was formed from continuous sheets of intercalate throughout the sample, either much of the intercalate within a layer would need to be removed from a sample before another stage could form or some stages would not be observed in the course of a reaction. In experiments with the

oxidation of graphite-potassium intercalation compounds, they observed that all stages were formed and that there was no indication of extensive rearrangement of the potassium to accomplish the change in stage. They proposed that these results could be explained if the intercalate was present in the sample as islands, i.e., rather than a layer of intercalate between nearest graphite planes and extending throughout the whole crystal, all planes of graphite could have an intercalate layer adjacent to them somewhere as long as staging was maintained locally. If the intercalate were present as islands on all graphite planes, then staging could occur by rearrangement of the islands without necessitating migration of the intercalate through the graphite planes or the skipping of stages.

Both of the terms "island" and "domain" have been used to describe the structure of the intercalate within graphite. The term "island" has generally been used to refer to a single layer of intercalate, bound by kinked layers of graphite at the edge of the intercalate. The term "domain" has been used by various workers to refer to a single layer of intercalate, an aligned three-dimensional stack of islands, and two-dimensionally ordered regions within an individual island. Within this paper, "island" is used to refer to a single layer of intercalate bounded by a dislocation loop with a Burgers vector normal to the basal plane, and "domain" is used to refer to a three-dimentional stack of islands showing a periodic structure perpendicular to the basal plane. Similarly, "domain wall" is used to refer to the dislocation loop array bounding a domain composed of intercalate islands.

The staging mechanism can be viewed as a balance of the interaction between the intercalate and the adjacent graphite layers and the repulsion of intercalate layers. Safran *et al.*[10,20,21] developed a theoretical explanation of the staging phenomenon based on electrostatic repulsion of intercalate islands due to the charge transfer from the intercalate to the adjacent graphite layers. When the pairwise interaction of the intercalate islands was taken into account, the phenomenon of staging arose as a means of minimizing the energy of the system. Millman and Kirczenow[12,22,23,24], Hawrylak and Subbaswamy [13] and Dahn *et al.*[25] further developed this theory of staging by including the influence of elastic strain energy on the energy of the system. Forgacs and Uiman[26] suggested a possible mechanism for a staging transition in intercalation compounds wherein the domain walls are rotated.

There are two distances which can be adjusted to balance the forces. These are the distance in the c-direction and the in-phase separation. The separation in the c-direction is a discrete function, since the islands have to be separated by multiples of the graphite layer thickness. In the plane the island separation can be varied continuously, although it is dependent on the balance between the intercalate potential outside the sample and the repulsion between islands within the sample. A potential gradient within the sample can be achieved by a variation in the in-plane spacing of the islands, with a change in stage occurring when one stage with a given inter-island spacing becomes unstable with respect to another stage with a different inter-island spacing (Fig. 1).

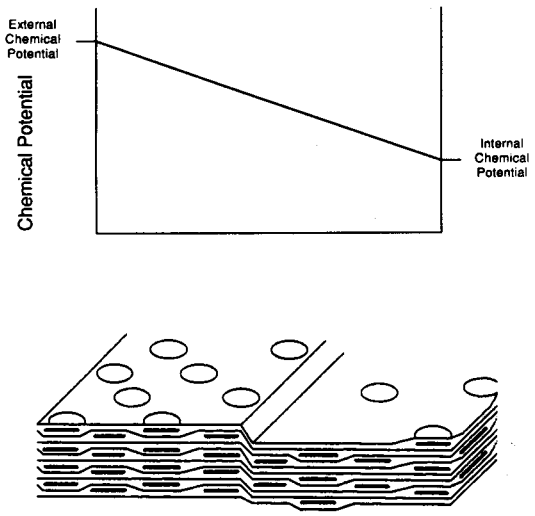

Fig. 1. Schematic representation of the potential gradient and island spacing. The upper panel shows the decrease in the potential gradient across the sample. The lower panel represents an increase in the spacing between intercalate islands going from left to right within the sample, with a change from stage 2 to stage 3 in the middle of the sample.

9. ESTIMATION OF RATE-LIMITING STEPS

Several scenarios are possible for the distribution of the intercalate within the sample during intercalation depending on the rate-limiting step. These scenarios are described in conjunction with Fig. 2, which schematically shows the chemical potential gradient within an intercalating sample under several types of reaction control. Fig. 2 (a) represents the intercalate distribution within the sample for all the rate-limiting cases. Outside the sample, the intercalate concentration is assumed to be uniform, and the concentration of the intercalate per unit volume in the vapor phase is assumed to be low. Immediately adjacent to the sample edge, stage s has formed. Further within the sample stage $s + 1$ has formed. Since intercalation compounds tend to have fairly pronounced stoichiometries, a step in the concentration profile exists at the interface between stage s and stage $s + 1$.

First, let us consider the case where transport external to the sample is rate-limiting, be it either evaporation from the intercalate reservoir, vapor phase transport, or condensation on the sample. This implies that both the diffusion within the sample and the staging reaction are fast compared to the trans-

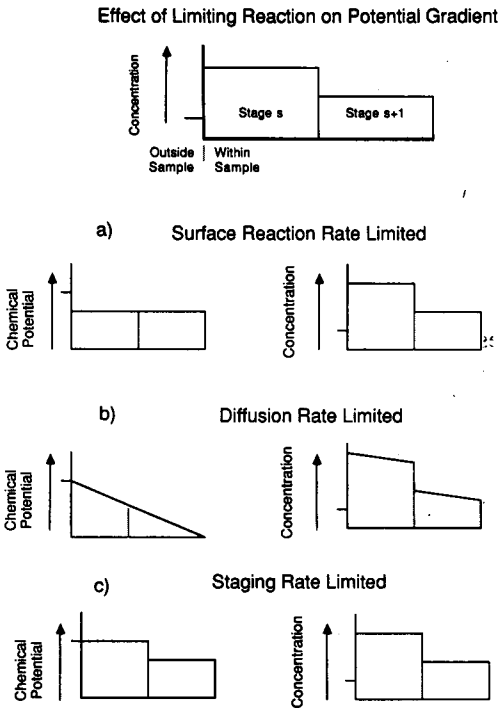

Fig. 2. Schematic of the profile of the chemical potential across the sample when the rate controlling step is (a) the surface reaction, (b) diffusion through the sample, or (c) the staging reaction.

port to the sample. Fast diffusion and staging mean that the intercalate should be able to distribute itself uniformly within the sample when the intercalate is available at the surface. A uniform concentration of intercalate across the sample implies that the overall concentration increases with time until the reaction is completed to the level allowed by the intercalate chemical potential. Stages should appear distinctly—initially a high stage throughout the sample, then a succession of stages with decreasing stage number, with two stages coexisting within the sample for only short periods of time. The chemical potential throughout the sample is constant, as illustrated by Figure 2 (b). A chemical potential gradient is only apparent at the sample surface, where the chemical potential of the intercalate vapor is larger than the chemical potential within the sample.

A second scenario is the case where transport to the sample is fast, as is the staging reaction, and diffusion within the sample is the controlling step. It was assumed that the chemical potential at the surface is constant throughout the intercalation period. In this case a chemical potential gradient exists between the edge of the sample and the central unintercalated region. In keeping with the concept of a potential gradient by gradual increase of the island separation, one would expect to see the final stage near the edge, with higher stages present as one progresses toward the center of the sample. This is illustrated in Fig. 2 (b), where only two stages are shown. While the intercalate potential at the sample edge is the same as the intercalate potential outside the sample, the chemical potential decreases within the sample until no intercalate is present. Hence one expects to see a mixture of stages present at nearly all times, with the amount of the higher stages being determined by the diffusion coefficient of each stage and the overall potential gradient. Physically, the sample can be expected to show the "window pane" or "ash tray" effect, i.e., the intercalated edges form a raised frame around the unintercalated center of the sample. This surface deformation is most noticeable when intercalating to low stage compounds because of the 50% or greater expansion which is characteristic of low stage intercalation compounds.

Finally, the staging reaction may also affect the morphology of the sample during intercalation. If it is assumed that different stages form at different rates, even though the growth of all the stages is limited by the staging reaction, the overall external appearance of the sample would be much like that observed in the diffusion-controlled case. The difference would be in the dependence of the intercalate front position as a function of time. The position of the interface between stages would be expected to vary as the square root of time if the reaction is diffusion-controlled, while the interface positions would be expected to vary linearly with time if the staging reaction shows first-order kinetics. A possible profile of the chemical potential during surface controlled intercalation is illustrated in Figure 2 (c), where the formation of stage $s + 1$ is slightly quicker than the rate of formation of stage s, with the result that the width of the $s + 1$ stage is increasing with time. Here again, only two stages are shown. In this example the chemical potential has the appearance of the concentration profile, since the chemical potential is only changing at the interface between stages.

The staging reaction can be considered a joint shift in the in-plane spacing of islands and in the c-direction repeat distance. Such a shift involves migration similar to that observed in the diffusion of the islands but over small distances and accompanied by a change in repeat distance. The activation energy of the staging reaction is expected to be similar to that of diffusion, since this view implies similar behavior in staging and in diffusion. However, the entropy change involved in diffusion and the staging reaction should be quite dissimilar, since staging is an ordering phenomenon and diffusion can be considered a disordering phenomenon. This implies that staging should be slower than diffusion. Diffusion in general may be quicker, but since diffusion occurs over fairly long distances, it can take a longer time than staging. An appropriate length for diffusion in general would be the width of the particular phase, while an appropriate length for the diffusion involved in staging would probably be on the order of one or two island diameters, or the width of the interface between stages. As long as the width of the interface can be

considered to be constant, the chemical potential gradient across the interface will be constant. With a constant potential gradient, the flux across the interface will be constant and the velocity of the interface will be constant.

Table 1 is a list of the parameters used to estimate the controlling reaction step for a variety of intercalates, culminating in Figure 3 which compares the relative significance of the different reaction steps in the overall reaction time. At the head of each column in Table 1 is the name of the intercalate; the leftmost column in the table is a description of the entry in that row.

The first seven rows contain physical constants of the intercalate which are used in further calculations. Row 1 lists the molecular weight of the vapor phase form of the intercalate. This is what would be expected from the chemical formulae except in the case of ferric chloride which exists as a dimer in the vapor phase. (The other metal chlorides also form dimers in the vapor phase, but to much lesser extents.) Rows 2 and 3 contain the melting point and boiling point of the intercalate, except in the case of palladium(II) chloride which sublimes rather than boiling. Similarly in Row 4 the value listed for palladium(II) chloride is the heat of sublimation rather than the heat of vaporization. The intermolecular separation listed in Row 5 was estimated as the cube root of the volume of the intercalate molecule in a unit cell of a solid phase of the material. The volume of the intercalate molecule was calculated by dividing the volume of the unit cell by the number of molecules in it.

The temperature given in Row 6 is the temperature at which it was assumed that the reaction takes place. Intercalation by a given species is not limited to that temperature; the value represents a temperature at which intercalation has been reported in the literature. For the purposes of these calculations, it is assumed that the sample and the source of the intercalate are at the same temperature. Consequently the temperature listed in Row 6 was used to calculate the vapor pressure listed in Row 7. The vapor pressure was calculated using the vapor pressure terms listed in Rows 24 through 26. The form of the equation used is

$$\log P = -A/T + B + CT + D \log T. \quad (14)$$

Values for the physical constants used in the first seven rows, as well as the constants in eq. (14) were obtained from tables listed in Ref. 23.

The terms listed in Rows 8 through 12 are associated with reaction steps external to the sample. The first of these is the evaporation rate of the intercalate from the source. The evaporation rate was calculated with eq. (2) in terms of the number of molecules evaporating per second. The transport time for the intercalate in the vapor phase can be obtained from eq. (6) using the interdiffusion coefficient listed in Row 9 and the molecular velocity listed in Row 10. If another gas is present, the interdiffusion coefficient tends to be the important term; otherwise the molecular velocity determines the transport time of the intercalate from the source to the sample. The inert gas pressure listed in Row 28 indicates whether or not additional gases are present in the intercalation system. The metal chlorides only intercalate graphite if an electron acceptor is present[27] or the metal chloride dissociates to form chlorine at the reaction temperature. For metal chlorides, the pressure listed in Row 28 is the larger of the minimum chlorine pressure necessary to intercalate and the dissociation pressure of chlorine at the intercalation temperature[28]. Bromine, iodine monochloride and nitric acid are assumed to be intercalated in air at a total pressure of 1 atm. The alkali metals and the pentafluorides are assumed to be intercalated in a vacuum of 10^{-6} torr.

The in-plane diffusion coefficient listed in Row 13 is estimated from empirical equations relating the self-diffusion coefficient of a material to its melting point. One of the two equations are used, depending on whether or not the intercalate possesses in-plane order at the intercalation temperature. In the case of an ordered intercalate, i.e. bromine and iodine monochloride, the equation used is [29]

$$D = 3.4 \times 10^{-5} T_m r_s^2 \exp\left[-17 \frac{T_m}{T}\right]. \quad (15)$$

where:

T_m is the melting point of the intercalate,
T is the intercalation temperature,
r_s is the intermolecular separation of the intercalate.

For disordered intercalates, the in-plane diffusion was assumed to be similar to self-diffusion of the molecule in liquid. The equation used is [30]

$$D = 3 \times 10^{-3} \exp\left[-7.2 \frac{T_m}{RT}\right]. \quad (16)$$

These empirical equations are used because diffusion coefficients are generally not available for intercalation compounds. The use of them assumes that movement of the intercalate islands within the sample is controlled by diffusion of the intercalate within an island.

Rows 14 through 17 list parameters relating to the intercalation compound formed. The layer thickness ratio in Row 14 is the ratio of the thickness of an intercalate layer to the thickness of an individual graphite plane. The ratios are based on the repeat distances published for the intercalation compounds[31] and assume a graphite layer thickness of 3.354 Å, which is based on a graphite d-spacing of

Table 1. Calculation of the reaction time for various reaction steps

Intercalate	Nickel(II) Chloride	Copper(II) Chloride	Palladium(II) Chloride	Arsenic Pentafluoride	Antimony Pentafluoride	Bromine	Iodine Monochloride	Nitric Acid	Potassium	Rubidium	Cesium	Iron(III) Chloride
1. Mass (g)	129.62	134.44	177.31	169.91	216.74	159.81	162.36	63.01	39.1	85.47	132.905	324.41
2. Melting point (°C)	1001	620	500	−80	8.3	−7.2	27.2	−42	63.2	38.9	28.4	306
3. Boiling point (°C)	1243	993	d	−53	141	58.78	97.4	83	756	688	678.4	315d
4. Heat of vaporization (kcal/mol)	53.41	46.3	33.5	5.02	10.8	7.064	9.876	9.42	19.39	18.11	19.4	32.7
5. Intermolecular separation (Å)	4.92	4.99	5.11	6.38	6.68	4.99	5.15	4.71	5.26	5.54	5.97	5.61
6. Temperature (°C)	600	600	600	25	90	25	25	25	270	300	300	270
7. Vapor pressure at T (torr)	0.08	22.50	2.11	600.00	114.20	217.13	24.64	61.13	0.10	1.13	2.17	59.56
8. Evaporation rate (#/sec)	1.06E + 13	6.03E + 14	7.82E + 17	1.22E + 22	1.57E + 19	8.33E + 20	6.52E + 18	2.96E + 19	4.61E + 18	2.16E + 19	4.46E + 18	5.81E + 12
9. Vapor diffusion coefficient (cm^2/sec)	70.810	2.063	58.162	0.275	1.745	0.357	0.334	0.444	7517.651	550.720	235.666	6.373
10. Molecular velocity (cm/sec)	9440.36	9269.58	8071.56	4818.23	4708.18	4968.16	4928.99	7912.11	13556.62	9419.05	7553.42	4706.44
11. # molecules hitting surface (#/sec)	7.94E + 18	2.31E + 21	1.88E + 20	9.36E + 22	1.43E + 22	3.49E + 22	3.93E + 21	1.57E + 22	2.32E + 19	1.79E + 20	2.77E + 20	4.98E + 21
12. Sticking coefficient	1.34E − 06	2.61E − 07	4.15E − 03	1.30E − 01	1.10E − 03	0.0239	0.0017	0.0019	0.1984	0.1204	0.0161	1.17E − 09
13. In-plane diffusion coefficient (cm^2/sec)	1.5E − 05	7.4E − 05	1.2E − 04	2.9E − 04	1.8E − 04	5.9E − 08	1.0E − 08	1.8E − 04	3.2E − 04	4.2E − 04	4.5E − 04	6.3E − 05
14. Layer thickness ratio (x/c)	1.77	1.80	1.98	1.51	1.52	1.10	2.13	1.34	0.61	0.69	0.77	1.79
15. Stage 1 stoichiometry (c:x)	5.5	4.9	4.9	8	8	7	4	5	8	8	8	9
16. Lowest stage	2	1	3	1	1	2	1	1	1	1	1	1
17. Moles intercalated	4.11E − 04	9.22E − 04	3.07E − 04	5.65E − 04	5.65E − 04	3.23E − 04	1.13E − 03	9.04E − 04	5.65E − 04	5.65E − 04	5.65E − 04	5.02E − 04
Reaction step times, assuming 4 mm × 12 mm × 0.5 mm sample, 30 cm vapor transport distance												
18. Evaporate time (sec)	2.37E + 07	9.37E + 05	2.41E + 02	2.84E − 02	2.21E + 01	2.37E − 01	1.06E + 02	1.87E + 01	7.51E + 01	1.60E + 01	7.76E + 01	5.29E + 07
19. Ext transport time (sec)	1.27E − 01	4.36E + 00	1.55E − 01	3.27E + 01	5.16E + 00	2.52E + 01	2.69E + 01	2.03E + 01	1.42E − 03	1.67E − 02	3.86E − 02	1.41E + 00
20. Condensation time (sec)	2.33E + 07	9.22E + 05	2.37E + 02	2.79E − 02	2.17E + 01	2.33E − 01	1.04E + 02	1.84E + 01	7.38E + 01	1.58E + 01	7.63E + 01	5.21E + 07
21. Internal diffuse time (sec)	2.64E + 03	5.43E + 02	3.30E + 02	1.39E + 02	2.21E + 02	6.79E + 05	4.01E + 06	2.21E + 02	1.26E + 02	9.58E + 01	8.96E + 01	6.35E + 02
22. Staging time (sec)	1.27E + 00	2.65E − 01	1.61E − 01	6.85E − 02	1.08E − 01	2.55E + 04	1.81E + 05	1.08E − 01	6.19E − 02	4.73E − 02	4.43E − 02	3.09E − 01
23. Total reaction time (sec)	4.69E + 07	1.86E + 06	8.08E + 02	1.72E + 02	2.70E + 02	7.04E + 05	4.19E + 06	2.78E + 02	2.75E + 02	1.28E + 02	2.44E + 02	1.05E + 08
24. Vapor pressure term A	11499	10119	7453	1094	2364	2047.75	2627	1986	4855	4010	3750	6499
25. Vapor pressure term B	12.051	12.941	8.86	7.845	8.567	8.65047	10.2024	8.447	11.41	7.05	6.88	13.74
26. Vapor pressure term C	0	0	0	0	0	0.0061	0	0	0	0	0	0
27. Vapor pressure term D	0	0	0	0	0	0.9589	0	0	−1.275	0	0	0

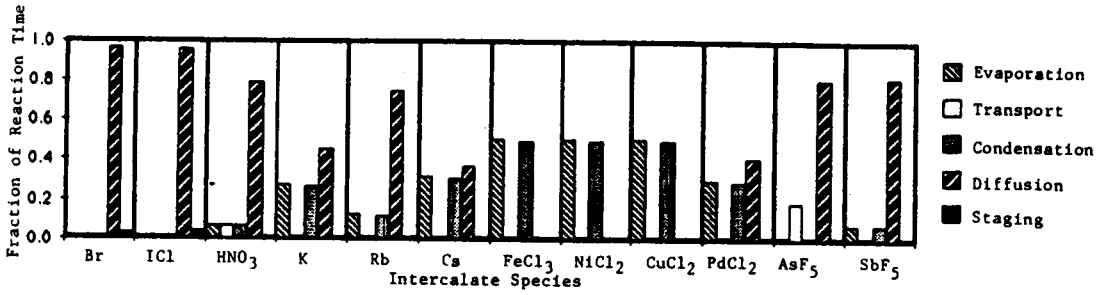

Fig. 3. A comparison of the significance of each reaction step calculated for several intercalate species.

6.078 Å. Row 15, labelled "Stage 1 Stoichiometry", indicates the in-plane stoichiometry commonly observed for the intercalate. This is the term, n, which is used to describe the stoichiometry of a stage s intercalation compound as $C_{sn}X$. The stage listed in Row 16 is the lowest stage observed for the intercalate, or equivalently in this case, the final stage reached at the intercalation temperature listed. Row 17 indicates the number of moles of intercalate necessary to intercalate a 4 mm × 12 mm × 0.5 mm sample to the stage listed in Row 16. (This size corresponds to the sample size used in an experimental study[32].) The number of moles of intercalate is used to calculate the time needed to evaporate and condense that amount of intercalate on the sample.

Rows 18 through 22 list the time necessary to complete a given step in the reaction, if that step were the only step involved. The calculations were made for a two-bulb case, with the sample and the source at the same temperature, but separated by 30 cm. The evaporation time listed in Row 18 is the length of time needed to evaporate the amount of intercalate listed in Row 17. Row 19 lists the time required for transport of the intercalate from the source to the sample. The transport time is calculated as the sum of the transport distance divided by the molecular velocity plus the transport distance squared divided by the vapor diffusion coefficient. The condensation time in Row 20 is calculated as the product of the inverse of the number of moles of intercalate striking the surface of the sample and the probability of the intercalate sticking to the sample after striking the surface.

Row 21 lists the time necessary for the intercalate to diffuse into the sample. This time is calculated as half the width of the sample, squared, divided by twice the in-plane diffusion coefficient listed in Row 13. The time can be approximated this simply because the interface between the intercalated region and the unintercalated region has a constant concentration.

The staging time listed in Row 22 was calculated assuming that the staging reaction was first order with respect to the intercalate and so could be ascribed a velocity of the form

$$v = 30 \exp\left[-Q\frac{T_m}{T}\right], \qquad (17)$$

where Q is the same empirical constant used in the in-plane diffusion coefficient, i.e., 17 for ordered intercalates, and 3.6 for disordered intercalates. The premultiplier was determined empirically from the experimental results for the intercalation of bromine in graphite by fitting the observed velocities on the upper branch of the time-temperature-transformation curves with eq. (17)[32].

Since a wide range of temperatures is considered, the times for an individual step vary over several orders of magnitude between the different intercalate species. To compare the relative importance of the individual reaction steps for the different intercalates, the reaction time for an intercalate is totaled and the amount of time relative to the total time is plotted as Figure 3. Several trends are evident from this figure. Bromine and iodine monochloride intercalate as ordered structures and consequently exhibit slow diffusion through the sample, with the result that diffusion control is expected. Intercalation of bromine in graphite was found to be diffusion-controlled under most conditions[32], and the length of time estimated for the reaction was on the order of what was observed.

The calculations for the alkali metals indicate that no single reaction step is clearly rate controlling. A better estimate of the individual reaction times could be obtained if a better understanding existed of the staging reaction and in-plane diffusion coefficients. The exact intercalation temperature and conditions also affects the reaction rates. Nonetheless, the implication of a mixture of controlling steps is supported by reports on the kinetics of alkali metal intercalation. Aronson and Salzano[33] indicated that the desorption of cesium from graphite intercalation compounds is controlled by the evaporation rate of cesium from the surface of the graphite. Pfluger *et al.*[34] indicated that the intercalation of alkali metals cannot be described adequately by a single reaction mechanism. Hamwi *et al.*[8] suggested that the kinetics of intercalation of potassium could be described by an empirical law of the form L = a exp(bt), where L is the penetration length of the intercalate, a is a normalization constant, b is the slope of the line defined by plotting ln L versus time, and t is the time.

The calculations for the metal halides indicate that the evaporation and condensation of the intercalate

on the sample are most likely the limiting reaction steps; this is consistent with the low vapor pressure at the reaction temperature. It may be possible to set up the reaction so that the metal halide is complexed with excess halogen to form a more volatile halide. If the halide complex decomposes at the sample surface, the net transport rate of the metal halide can be increased[35,36]. Such a complexing reaction is not taken into account in this approximation of the transport step. Nonetheless, Flandrois[37] investigated the intercalation of nickel chloride and concluded from the kinetics and the activation energy that the reaction controlling step was either evaporation or condensation. The same conclusion was reached by Dowell and Badorrek[6] in a study of the intercalation of palladium chloride in graphite.

Nitric acid, arsenic pentafluoride and antimony pentafluoride form a special group. For these compounds the active intercalating agent is formed by the dissociation of the initial intercalate. Forsman[38] proposed for nitric acid that the dissociation of the nitric acid molecule was necessary before reaction with graphite could occur (eq. (18)).

$$2\,HNO_3 = NO_2^+ + NO_3^- + H_2O. \quad (18)$$

Similarly, eq. (19) was proposed for the dissociation of pentafluorides during intercalation[39]:

$$3\,MF_5 + 2\,e^- = 2\,MF_6^- + MF_3 \quad (19)$$

where:

M stands for the metal involved.

Figure 3 indicates that all three compounds (HNO_3, AsF_5, SbF_5) should be diffusion controlled. However, the analysis ignores the possibility of a surface reaction other than adsorption, and is therefore probably not appropriate for these compounds which undergo dissociation. Experimentally it does seem that for these compounds a surface reaction may be the limiting step. Forsman indicated that a surface reaction may be the controlling step in the intercalation of nitric acid[4]; Hooley[40] observed that the intercalation rate of arsenic pentafluoride is markedly different between the first intercalation rate and that obtained by desorbing the sample and subsequently re-intercalating.

The calculated effect of varying the temperature of the system, or having the intercalate source and sample at different temperatures is indicated in Fig. 4. This figure illustrates the change in the relative importance of the reaction steps for the intercalation of cesium under various conditions. Reaction times were calculated for source temperatures of 250, 300, 350 and 400°C, with source-sample temperature differences of 0, 50 and 100°C for each source temperature. The primary effect of an increased temperature is to increase the relative importance of the diffusion step in the reaction. This is the result of an activation energy for diffusion which is smaller than the heat of vaporization. As the temperature is increased, the vapor pressure of cesium increases more rapidly than the diffusion rate. On the other hand, as the temperature difference between the source and the sample is increased, the diffusion rate of the intercalate within the sample is increased while the intercalate pressure is not changed.

10. ON PREDICTING CONTROLLING FACTORS

In general, the principle factors in determining the intercalation rate appear to be the diffusion rate of the intercalate within the sample and the vapor pressure of the intercalate. A low vapor pressure of the intercalate implies slow evolution times of the intercalate from the source and rate-limiting steps external to the sample. Surface reactions may also be rate-limiting, but are very difficult to estimate *a priori*.

In the case of graphite-iron chloride, Metz and Seimsgluss[3] suggest a combination of a diffusion rate with a $t^{1/2}$ dependence and a rate with a linear time dependence. They suggested that the linear rate is a function of nucleation of intercalate islands at the graphite edges. They observed a shift in the controlling step by comparing the intercalation rates in fibers with the intercalation rate in HOPG. In the fibers they found the linear term to be dominant, while the diffusion term dominates the rate in HOPG. This is similar to the results obtained by

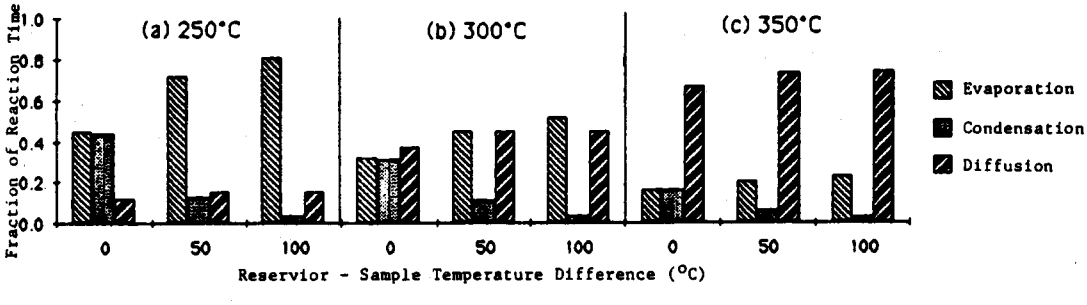

Fig. 4. The effect of a difference in the sample temperature and the intercalate reservoir temperature on the intercalation rate.

Ubbelohde *et al.*[7] in the graphite-bromine system, which showed that the reaction rate decreased as the quality of the graphite decreases. Furthermore, Hooley[41] indicated that graphite-iron chloride is quite sensitive to the crystal stress state when he observed that graphite flakes become only partially intercalated with iron chloride from nitromethane solutions. The arguments[3] that the linear term is due to the nucleation rate at the sample edge rather than the staging reaction rate is not particularly compelling. For example, for graphite-bromine, observation of edge expansion indicates that the edge of the sample appears to be completely intercalated at very short times relative to the length of time needed for the whole sample[42]. However, in some systems the growth at the edge of the sample may well be the controlling term[24].

In graphite-nickel chloride, Flandrois suggested that the kinetics which were actually observed were related to sublimation or adsorption of the nickel chloride rather than intercalation per se. This conclusion was based on the fact that the activation energy observed for the reaction was essentially the same as that expected for a metal halide. It was observed by X-ray diffraction peak broadening that the islands were about 100 Å in diameter while the excess chloride present in the stoichiometry suggested that the islands were approximately the minimum size allowable. The small island size implies that, in this case, complete islands were formed at the sample edge, which then diffused through the sample as soon as the islands were large enough for the decrease in volume free energy accompanying the reaction to be larger than the increase in energy due to the island boundary. The small island size observed and the uniform staging also suggest that the reaction rate is controlled by transport to the sample.

A particular problem in looking at the kinetics of intercalation is the selection of intercalation conditions which allow the reaction to be controlled by the intercalation rather than by the transport of the intercalate to the sample. For example, nitric acid has been studied by weight uptake and diffusion coefficients have been assigned to account for the reaction rate[6,43]. However, other studies have indicated that reactions at the surface are controlling[4,38,44].

In this work the reaction rate of nitric acid with highly oriented pyrolytic graphite was found to increase by a factor of 10 by changing the intercalation conditions from vapor transport to immersion in liquid nitric acid. Figure 5 illustrates the difference in the rate which can be produced by the difference in intercalation conditions. X-ray absorption in air using Cu K*a* radiation in transmission (Appendix) was used to measure the concentration profile of nitric acid perpendicular to the *c*-axis in partially intercalated graphite. The filled circles indicate the concentration profile of nitric acid in graphite after immersion in red fuming nitric acid for 2 min. The open circles indicate the concentration profile of nitric acid in graphite after exposure to red fuming nitric acid for 28 min. The amount of unintercalated graphite was about the same in the two samples, and the nitric acid concentration in the immersed sample was approximately twice of that of the sample exposed to vapor. Similarly, concentration profiles indicated that no unintercalated graphite remained after liquid intercalation for 5 min or vapor intercalation for 50 min. Both liquid and vapor intercalation resulted in a final stage of 4, but the liquid intercalation sample showed fourth stage X-ray diffraction peaks during intercalation while the vapor intercalated sample showed predominantly higher stages even after 50 min. Concurrent with the reaction rate increase was a change in the sample morphology during the reaction. During intercalation in nitric acid vapor, the sample rarely showed the window pane deformation common to graphite-bromine. On immersion however, the window pane type of deformation was clearly observed. This suggests that a clue to the controlling step in the reaction may be obtained from the deformation accompanying intercalation. Namely, if the surface does not appear to deform (as in vapor phase HNO_3 intercalation), it is likely that staging is fairly uniform across the sample which implies that the reaction is limited before the intercalate reaches the sample, or in the adsorption step. On the other hand if surface deformation is pronounced (as in liquid phase HNO_3

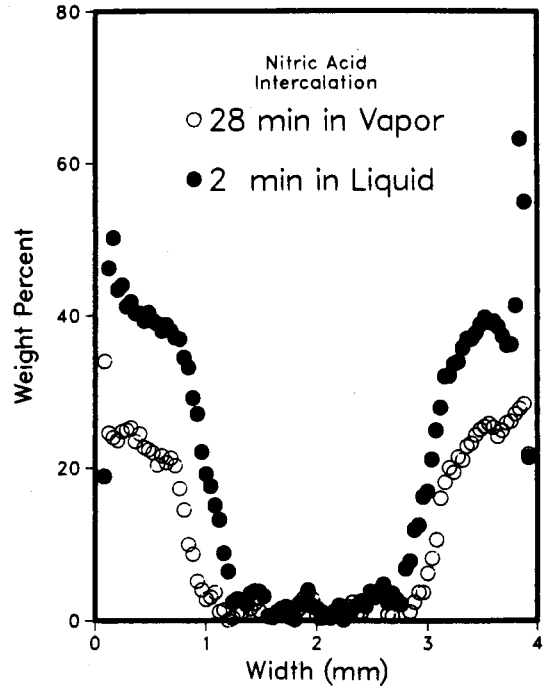

Fig. 5. Concentration profiles of nitric acid in graphite. The filled circles indicate the nitric acid concentration in HOPG immersed in nitric acid for 2 min at room temperature; the open circles indicate the nitric acid concentration profile in HOPG exposed to nitric acid vapor for 28 min.

Table 2. Mass absorption coefficients of HNO_3 and C

μ/ρ (cm^2/g)[46]	HNO_3	C
Cu Kα	9.97	4.22
Layer density (g/cm^3)	1.80	2.27
Stoichiometry at saturation	$C_5 NO_3^- \cdot HNO_3$[38]	—
Stage at saturation	1	—

intercalation), it is likely that multiple stages are present with diffusion limiting the reaction rate.

The model of the reaction steps presented here ignores the effect of surface reactions on the kinetics because there is no general surface reaction to be modeled. Nonetheless, a surface reaction can readily be rate controlling and many intercalating agents may be susceptible to the effect of surface reactions on the intercalation rate. As another example, metal halides typically have a very low vapor pressure at temperatures where low stage compounds are formed. As a result, the transport rate of the metal halide to the sample is too slow to allow reasonable reaction times. A method of increasing the transport rate is to complex the halide with a halogen to form more volatile halides. The vapor phase transport rate of the halide may increase, but it may also be possible that the dissociation of the metal complex at the sample surface can become rate limiting. Alternately, there may be other reactions at the intercalate surface which compete for the intercalating species. Hooley suggested that this may be the case in the intercalation of bis-(chlorosulfuryl) peroxide[45]. Vapor phase intercalation of nitric acid may also be affected by competing surface reactions, given that water can be formed on the surface of the sample as a by-product of the reaction due to the hygroscopic nature of nitric acid.

Ulloa and Kirczenow[24] proposed a theory of interaction between intercalate domain walls which implies that certain compounds form slowly because of size constraints. The theory was qualitative in the sense that it did not predict reaction rates, but rather indicated which species may be expected to form with difficulty. The model proposed in this paper is complimentary to the Ulloa and Kirczenow paper in that our model estimates the factors affecting the reaction rate under the conditions where Ulloa and Kirczenow do not predict difficulties.

Acknowledgments—The X-ray diffraction equipment grant from the Division of Materials Research of the National Science Foundation under Grant DMR-8005380 was essential for this work. Equipment support from the Materials Research Laboratory Section, Division of Materials Research, National Science Foundation, under Grant DMR-76-81561 A01 is also acknowledged.

REFERENCES

1. J. G. Hooley, *Mater. Sci. Eng.* **31**, 17 (1977).
2. K. K. Bardhan and D. D. L. Chung, *Carbon* **18**, 303 (1980).
3. W. Metz and L. Siemsgluss, *Mater. Sci. Eng.* **31**, 119 (1977).
4. T. Dziemianowicz, K. Leong and W. C. Forsman, *Mat. Res. Soc. Symp., Proc.* Vol. 20, *Intercalated Graphite*, Elsevier, p. 277 (1983).
5. M. B. Dowell, *Mater. Sci. Eng.* **31**, 129 (1977).
6. M. B. Dowell and D. S. Badorek, *Carbon* **16**, 241 (1978).
7. G. A. Saunders, A. R. Ubbelohde and D. A. Young. *Proc. Roy. Soc.* **A 271**, 512 (1963).
8. A. Hamwi, P. Touzain, L. Bonnetain, A. Boeuf, A. Freund and C. Riekel, *Mater. Sci. Eng.* **57**, 161 (1983).
9. R. Nishitani, Y. Uno and H. Suematsu, *Phys. Rev.* **B 27**, 6572 (1983).
10. S. A. Safran and D. R. Hamann, *Phys. Rev. Lett.* **42**, 1410 (1979).
11. S. A. Safran, P. S. Sahni and G. S. Grest, *Phys. Rev.* **B 28**, 2693 (1983).
12. G. Kirczenow, *Phys. Rev. Lett.* **55**, 2810 (1985).
13. P. Hawrylak and K. R. Subbaswamy, *Phys. Rev. Lett.* **53**, 2098 (1984).
14. S. Dushman, *Scientific Foundations of Vacuum Technique*, Wiley, New York (1962).
15. H. Eyring, F. M. Wanlass, E. M. Eyring, *Condensation and Evaporation of Solids*, E. Rutner, P. Goldfinger and J. P. Hirth, eds., 1964, Gordon and Breach, p. 3.
16. S. R. Shatynski, J. P. Hirth and R. A. Rapp, *Acta Met.* **24**, 1071 (1976).
17. A. Herold, *Proc. of the 10th International Symp. on the Reactivity of Solids*, P. Barret and L. X. Dufour, eds., Elsevier, p. 461 (1985).
18. S. Aronson, *J. Inorg. Nucl. Chem.* **25**, 907 (1963).
19. N. Daumas and A. Herold, *C. R. Acad. Sci.* **C 268**, 373 (1969).
20. S. A. Safran, in *Domain Structures in Graphite Intercalation Compounds*, Springer Verlag, 1981 Series in Solid State Science Vol. 38, p. 43.
21. S. A. Safran, P. S. Sahni and G. S. Grest, *Phys. Rev.* **B 26**, 466 (1982).
22. S. E. Millman and G. Kirczenow, *Phys. Rev.* **B 26**, 2310 (1982).
23. S. E. Millman and G. Kirczenow, *Phys. Rev.* **B 28**, 3482 (1983).
24. S. E. Ulloa and G. Kirczenow, *Phys. Rev. Lett.* **55**, 218 (1985).
25. J. R. Dahn, D. C. Dahn and R. R. Haering, *Solid State Comm.* **42**, 179 (1982).
26. G. Forgacs and G. Uiman, *Phys. Rev. Lett.* **52**, 633 (1984).
27. G. K. Wertheim, *Solid State Comm.* **38**, 633 (1981).
28. R. Colton and J. H. Canterford, *Halides of the First Row Transition Metals*, Wiley-Interscience (1969).
29. J. Askill, *Tracer Diffusion Data for Metal Alloys and Simple Oxides*, IFI/Plenum (1970).
30. L. Nanis and J. O'M. Bokris, *J. Phys. Chem.* **67**, 2865 (1963).
31. A. Herold, in *Physics and Chemistry of Materials with Layered Structures*, F. Levy, ed., D. Reidel Publishing Company, Dordrecht, Holland, Vol. 6, Intercalated Layered Materials, p. 323 (1979).
32. S. H. Anderson Axdal and D. D. L. Chung, *Carbon* **25**, 191 (1987).
33. F. J. Salzano and S. Aronson, *J. Chem. Phys.* **42**, 1323 (1965).
34. P. Pfluger, V. Geiser, S. Stolz and H.-J. Guntherodt, *Synth. Met.* **3**, 27 (1981).
35. H. Schafer, *Chemical Transport Reactions*, Academic Press (1964).
36. T. S. Dziemianowicz, R. Vangelisti, A. Herold, and W. C. Forsman, *Carbon* **22**, 53 (1984).
37. S. Flandrois, J. M. Masson, J. C. Rouillon, J. Gaultier and C. Hauw, *Synth. Met.* **3**, 1 (1981).
38. W. C. Forsman, F. L. Vogel, D. E. Carl and J. Hoffman, *Carbon* **16**, 269 (1978).

39. N. Bartlett, B. McQuillan and A. S. Robertson, *Mat. Res. Bull.* **13**, 1259 (1978).
40. J. G. Hooley, *Carbon* **22**, 217 (198).
41. J. G. Hooley, in *Physics and Chemistry of Materials with Layered Structures*, R. M. A. Lieth, ed., Reidel, Vol. 1, 1973, p. 16.
42. K. K. Bardhan, J. C. Wu, J. S. Culik, S. H. Anderson and D. D. L. Chung, *Synth. Met.* **2**, 57 (1980).
43. M. B. Dowell, *Ext. Abstr. and Prog.*, 13*th Bienn. Conf. Carbon*, p. 136 (1977).
44. S. R. Su and D. W. Oblas, *Mat. Res. Soc. Symp., Proc. Vol.* 20, *Intercalated Graphite*, Elsevier, p. 231 (1983).
45. J. G. Hooley, *Ext. Abstr and Prog.*, 16*th Bien. Conf. Carbon*, p. 240 (1983).
46. R. C. Weast, editor, *Handbook of Chemistry and Physics*, Chemical Rubber Company, Vol. 54 (1974).

APPENDIX

Most intercalates may be readily measured by x-ray absorption because of the large difference between the mass absorption coefficient of carbon and that of the intercalate. Since the thickness of the graphite layers is essentially constant, comparing the ratio of the transmitted to incident beam before and after intercalation allows a rather accurate determination of the intercalate concentration.

A description of the geometry of the absorption set-up follows. The Siemens diffractometer was set at a 2θ value of 0°. The normal sample holder held a collimating slit constructed of two glass plates separated by a copper foil so as to form a slit of size 10 μm by 2 mm. The absorption sample was held with its basal plane perpendicular to the beam 2 cm from the slit. The sample was translated through the beam by a synchronous motor turning a micrometer. A 0.1 mm slit was located 13 cm from the sample before a monochromator and scintillation detector. The dead time of the detector was determined to be 10 μs. Although the sample moved continuously, the intensity was measured as the number of counts in periods of 1.6 s each. Counting was begun before the sample intercepted the beam and was continued until after the sample was fully out of the beam. The intensity measured before and after the sample intercepted the beam was averaged to serve as the incident beam intensity. Cu K*a* radiation was used with a graphite monochromator.

The absorbance of the transmitted beam may be calculated with the following equation:

$$\left(\frac{I}{I_o}\right)^{\lambda} = \exp-[\mu_a^{\lambda}X_a + \mu_b^{\lambda}x_b + \mu_c^{\lambda}x_c + \ldots], \quad (20)$$

where I_o is the unabsorbed beam intensity, I is the transmitted beam intensity, μ_a^{λ} is the linear absorption coefficient of component a (a = C or HNO_3) at wavelength λ, and x_a is the thickness of component a. The values of relevant quantities are listed in Table 2. When a single intercalate was present, a weighted average of the absorption coefficients of the intercalate and carbon was used in the calculations. This is tantamount to assuming that the intercalate species is present in molecular form. The value of x_a is constant for a = graphite, otherwise x_a is the thickness of the intercalate present. Hence the concentration of component a can be determined knowing the initial graphite thickness and the amount of expansion in the c-direction resulting from a given stage compound. Using the nominal expansion of a first stage compound as the expected expansion, higher stages can be represented as concentrations equal to the reciprocal of the stage number. Since the graphite layer thickness remained constant for a given sample, the intercalate composition could be determined if the absorption profile of the graphite was obtained before intercalation was begun.